BLIND TIMING ACQUISITION FOR ULTRA-WIDEBAND MULTI-USER AD HOC ACCESS

Xiliang Luo and Georgios B. Giannakis

Department of ECE, University of Minnesota
200 Union Str. SE, Minneapolis, MN 55455

ABSTRACT

Synchronization is a factor critically affecting performance of ultra-wideband (UWB) communication systems. We develop a blind synchronization and demodulation scheme which relies on intermittent transmission of nonzero mean symbols. These enable multi-user interference (MUI)- and inter-symbol interference (ISI)-resilient timing acquisition via energy detection and low-complexity demodulation by matching to a synchronized aggregate template (SAT). It turns out that the resultant SAT receiver offers distinct advantages over the widely-deployed RAKE receiver. Its blind operation nicely fits the requirements of multi-user ad hoc access and its ability to handle ISI and MUI is attractive for UWB communications. Analytical performance evaluation and simulations testing our novel scheme confirm its high potential for deployment.

1. INTRODUCTION

Having as goal the timing of symbol boundaries, synchronization is the first module of any coherent receiver, and thus plays a critical role in ensuring reliable communications. Timing becomes more challenging with wideband (WB) transmissions over frequency-selective channels which induce intersymbol interference (ISI), especially in multiple access links where one must also deal with multiuser interference (MUI). Synchronization challenges are magnified with ultra-wideband (UWB) transmissions where ISI effects are particularly pronounced, causing bit error rate (BER) performance to degrade severely due to mis-timing [1], and capacity to diminish when timing offset as well as channel coefficients and tap delays can not be acquired [2]. Most UWB synchronizers rely on training, some assume absence of ISI [3], sampling rates as high as several GHz [4], or absence of MUI [5]. Without ISI and MUI, interesting data-aided and blind algorithms have been developed recently in [6], where UWB receivers acquire Timing via Dirty-Templates (TDT) formed from the received noisy waveform; see also [7] and [8]. However, blind TDT schemes require long data records and are available only for single-user links. In multi-access scenarios, performance degrades markedly in the presence of MUI, which turns out to be another major performance-limiting factor when many asynchronous communicators are to be synchronized, even with data-aided TDT. In a nutshell, there is a need for simple and preferably blind synchronizers flexible to operate with transmissions over additive white Gaussian noise (AWGN) or multipath channels, in single- or multi-user settings designed for fixed or ad hoc access.

This work was supported through collaborative participation in the Communications and Networks Consortium sponsored by the U. S. Army Research Laboratory under the Collaborative Technology Alliance Program, Cooperative Agreement DAAD19-01-2-0011.

In the present paper, we aspire to fill this need by introducing transmission protocols and low complexity receiver processors capable of ISI- and MUI-resilient timing acquisition and coherent demodulation. We will state the problem and lay out preliminary notions of our protocol in Section 2. Section 3 will deal with timing acquisition and recovery of what we term synchronized aggregate template (SAT) that incorporates the transmit-filter convolved with the ISI channel. We analyze the performance of our SAT estimators and demodulators in Section 4. Corroborating simulations are provided in Section 5, to confirm our conclusions in Section 6 and testify that our novel schemes have great potential for deployment.

2. PRELIMINARIES AND PROBLEM STATEMENT

Consider the ad hoc network configuration in Fig. 1, where node A is broadcasting with period T_s information bearing symbols $s(n)$ by linearly modulating the transmit (spectral shaping) pulse $p_T(t)$ of duration $T_T \leq T_s$. With $\mathcal{E}$ denoting energy per symbol, the transmitted waveform is:

$$u(t) = \sqrt{\mathcal{E}} \sum_n s(n) p_T(t - nT_s) \; . \tag{1}$$

This transmission can be intended to a single receiving node (point-to-point link) or even to multiple ones. For low-duty cycle UWB systems, $p_T(t) = \sum_{k=0}^{N_f-1} p(t - kT_f - c_k T_c)$, where $p(t)$ denotes a unit-energy pulse (a.k.a. monocycle) of duration $T_p < T_c$ (in the order of 1ns giving rise to GHz bandwidth); $T_f = N_c T_c$ is the duration of a frame comprising N_c chips; $\{c_k\}_{k=0}^{N_f-1} \in [0, N_c - 1]$ is a time hopping code[1] shifting the pulse to user-specific positions; and N_f is the number of frames (pulses) per information symbol. Here, we have $T_T = (N_f - 1)T_f + c_{N_f-1}T_c + T_p \leq T_s = N_f T_f$; see e.g., [8]. In UWB transmissions symbols are typically BPSK with $s(n)$ taking ± 1 values equiprobably.

The multipath channel between any two nodes is allowed to be frequency-selective (and thus ISI-inducing) with impulse response $\sum_{l=0}^{L} \alpha_l \delta(t - \tau_l)$, where taps $\{\alpha_l\}_{l=0}^{L}$ and delays $\{\tau_l\}_{l=0}^{L}$ are assumed invariant over a block of symbols (block fading model). Typically, the channel's coherence time (T_{coh}) satisfies: $T_{coh} \gg T_s$. Letting $\tau_{l,0} := \tau_l - \tau_0$, isolates the direct-path delay τ_0 which creates the timing offset between transmitter and receiver, and leads to the channel:

$$h(t) = \sum_{l=0}^{L} \alpha_l \delta(t - \tau_{l,0}). \tag{2}$$

Channel- and transmit-filter effects are combined in the received symbol waveform $p_R(t)$ of duration $T_R := \sup\{t | p_R(t) \neq 0\}$,

[1]Here we set $c_0 = 0$ to ensure that $\inf\{t | p_T(t) \neq 0\} = 0$. This is without loss of generality (w.l.o.g.), since we can incorporate $c_0 T_c$ into the unknown channel delay.

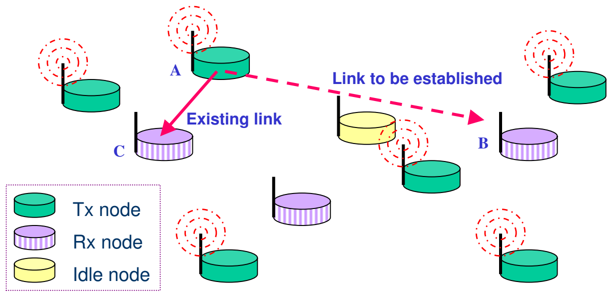

Fig. 1. A multi-access ad hoc configuration (cluster topology).

where $p_R(t) := p_T(t) \star h(t) = \sum_{l=0}^{L} \alpha_l p_T(t - \tau_{l,0})$, with $\star$ denoting convolution.

At a receiving node, we observe $u(t) \star h(t - \tau_0)$ in the presence of MUI $\rho(t)$ and AWGN $\eta(t)$. The latter has two-sided power spectral density $N_0/2$ and bandwidth W dictated by the low-pass front-end filter's cutoff frequency; i.e., the received waveform is [c.f. (1) and (2)]

$$r(t) = \sqrt{\mathcal{E}} \sum_n s(n) p_R(t - nT_s - \tau_0) + \eta(t) + \rho(t) \ . \quad (3)$$

Given only $r(t)$, we seek a transmission protocol equipped with a synchronization pattern enabling low-complexity blind estimation of τ_0, $p_R(t)$ and detection of $s(n)$ in the presence of noise, MUI and ISI. Towards this objective, we will adopt the following operating conditions:

C1: *We choose the symbol period $T_s > \Delta\tau_{\max} - T_T$, where $\Delta\tau_{\max} \geq \max_{l\in[1,L]}(\tau_l - \tau_{l-1})$ denotes a known upper bound on successive path delay differences.*

C2: *With the delay spread $\tau_{L,0}$ (and thus $T_R = T_T + \tau_{L,0}$) known, we select an integer $M := \lceil T_R/T_s \rceil + 1$.*

C3: *During synchronization, every $M - 1$ zero mean symbols $s(n)$ we transmit one nonzero mean symbol; i.e., writing $n = kM + m$ with $m \in [0, M-1]$, our symbol stream $\{s(n)\}$ taking values from a finite alphabet equiprobably, will obey: $\mathsf{E}[s(kM+m)] = \mu_0 \delta(m)$ with $\mu_0 \neq 0$. Outside the synchronization interval, symbols are zero-mean throughout: $\mathsf{E}[s(n)] = 0 \ \forall n$.*

C4: *The MUI in (3) is zero mean: $\mathsf{E}[\rho(t)] = 0$.*

Condition C1 ensures that over the $[0, T_R]$ support of $p_R(t)$, intervals where $p_R(t) = 0$ are no larger than T_s - a condition whose usefulness will become clear soon. For clarity in exposition we rely on exact knowledge of $\tau_{L,0}$ in C2. However, we have shown that all our ensuing results carry over with an upper bound too [9].

Notice also that in C3 we transmit a limited number of symbols (1 out M) with nonzero mean and only during the synchronization phase; otherwise, we rely on zero mean constellations that are power efficient. To maintain the same demodulator for zero-mean and nonzero mean symbols, we will effect the nonzero-mean property by minimally biasing the amplitude of certain constellation points. For instance, we can use *asymmetric BPSK* with nonzero-mean: $\mu_0 = \mathsf{E}[s(kM)] = 0.5\theta + 0.5(-1)$, where $\theta > 1$. If the receiver can only "hear" a single transmitter broadcasting the nonzero mean synchronization pattern, then C4 is satisfied regardless of how many zero-mean interfering signals from other communicating nodes are present. This is the case with star or clustered topologies of ad hoc networks, where a single (but not always the same) node undertakes the task of synchronizing neighbors.

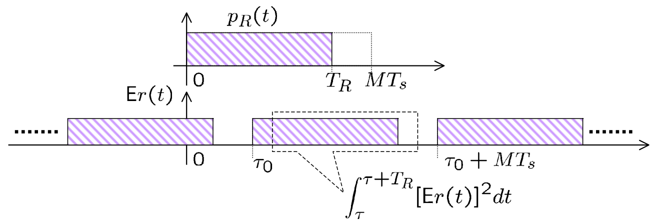

Fig. 2. Schematic illustrating the energy detector used for timing estimation.

3. BLIND SYNCHRONIZATION AND DEMODULATION

Under C3 and C4, the mean of the received waveform in (3) is:

$$\mathsf{E}r(t) = \sqrt{\mathcal{E}}\mu_0 \sum_n p_R(t - nMT_s - \tau_0) \ . \quad (4)$$

Because $\mathsf{E}r(t)$ is periodic with period MT_s, eq. (4) establishes that $r(t)$ exhibits cyclostationarity also in its mean. A period of the latter can be estimated using the mean-square sense (mss) consistent sample average across N segments of $r(t)$ each of size MT_s [10]:

$$\bar{r}(t) = \frac{1}{N} \sum_{n=0}^{N-1} r(t + nMT_s), \quad t \in [0, MT_s]. \quad (5)$$

Relying on $\mathsf{E}r(t)$ (or $\bar{r}(t)$ in practice), we will see next how we can first recover a synchronized aggregate template (SAT) of $p_R(t)$ that will subsequently allow us to demodulate.

3.1. SAT Recovery

Notice that our choice in C2 implies that over any interval of size MT_s, the mean $\mathsf{E}r(t)$ in (4) contains a circularly shifted (by τ_0) copy of $p_R(t)$ which has support of size $T_R \leq (M-1)T_s$. In fact, if τ_0 were known, then the desired SAT would be readily obtained as

$$p_R(t) = \frac{1}{\sqrt{\mathcal{E}}} \frac{1}{\mu_0} \mathsf{E}r(t + \tau_0), \quad t \in [0, T_R]. \quad (6)$$

To find τ_0, we will exploit the zero-guards of size $MT_s - T_R \geq T_s$ present in each period of $\mathsf{E}r(t)$; see Figure 2. To this end, let τ be a candidate shift (timing offset) which w.l.o.g. we confine to $[0, MT_s)$ as per (4). With $\tau \in [0, MT_s)$, consider the objective function: $J(\tau) := \int_0^{T_R} [\mathsf{E}r(t+\tau)]^2 dt$, which for the correct timing $\tau = \tau_0$ extracts the whole energy of $p_R(t)$; i.e., $J(\tau_0) = \mathcal{E}\mu_0^2 E_R$, where $E_R := \int_0^{T_R} p_R^2(t)dt$ denotes the SAT energy. We will show that τ_0 is the *unique* maximum of $J(\tau)$. Specifically, if $\tau > \tau_0$, only the periods corresponding to $n = 0, 1$ in (4) will appear[2] in $J(\tau)$, yielding $J(\tau) = \mathcal{E}\mu_0^2[\int_0^{T_R} p_R^2(t + \tau - \tau_0)dt + \int_0^{T_R} p_R^2(t - MT_s + \tau - \tau_0)dt]$. Recalling that $p_R(t) = 0$ for $t \notin [0, T_R]$, we obtain $J(\tau) = \mathcal{E}\mu_0^2[\int_{\tau-\tau_0}^{T_R} p_R^2(t)dt + \int_0^{\tau-\tau_0-(MT_s-T_R)} p_R^2(t)dt]$, which can be re-written as (see also Fig. 2):

$$J(\tau) = J(\tau_0) - \int_{\tau-\tau_0-(MT_s-T_R)}^{\tau-\tau_0} p_R^2(t)dt. \quad (7)$$

Because of C1, the integral in the right hand side is lower bounded by the positive quantity $\int_{\tau-\tau_0-T_s}^{\tau-\tau_0} p_R^2(t)dt$ when $\tau - \tau_0 > 0$. This implies that for $\tau > \tau_0$ (and likewise for $\tau < \tau_0$), we have $J(\tau) < J(\tau_0) \ \forall \tau \neq \tau_0$, and therefore:

$$\tau_0 = \arg \max_{\tau\in[0,MT_s)} J(\tau) \ , \ J(\tau) := \int_0^{T_R} [\mathsf{E}r(t+\tau)]^2 dt \ . \quad (8)$$

[2] Likewise, if $\tau < \tau_0$ then $n = -1, 0$ and being completely analogous to those with $\tau > \tau_0$ the subsequent steps of the proof for $\tau < \tau_0$ are omitted.

Using (5) to replace ensemble- with sample-mean estimates in (8) and (6), establishes the main result of this subsection on blind synchronization and SAT recovery, which we summarize next.

Proposition 1: *Under C1-C4, the timing offset* τ_0 *and the SAT* $p_R(t)$ *can be estimated blindly in the presence of ISI and MUI using*

$$\begin{aligned}\hat{\tau}_0 &= \arg \max_{\tau\in[0,MT_s)} \int_0^{T_R} \bar{r}^2((t+\tau)_{\text{mod } MT_s})dt \; ; \\ \hat{p}_R(t) &= \frac{1}{\sqrt{\mathcal{E}}}\frac{1}{\mu_0}\bar{r}(t+\hat{\tau}_0), \;\; t\in[0,T_R] \, , \end{aligned} \tag{9}$$

where the $(\text{mod } MT_s)$ *operation is used because* $\bar{r}(t)$ *in (5) is estimated over a period of size* MT_s *whereas the integration in (9) needs its periodic extension.*

Notice that no available approach can acquire timing of UWB transmissions in the generic setting allowed herein. Neither information bearing transmission must be interrupted for training nor transmit-filters, channels or spreading codes need to be known, so long as they remain invariant while averaging in (5) is performed. Contrary to all existing approaches, our estimators in (9) bypass channel estimation and instead acquire the timing offset and the *continuous-time* SAT – a step leading to improved demodulation as will see in the next subsection. A remark is due before that.

Remark 1: Although training is to be avoided in ad hoc access, if available in a point-to-point link, we can take M odd and alternate our $M-1$ zero-mean ± 1 symbols per synchronization period so that their mean is deterministically zero. For a given accuracy, this will require a smaller N in the sample average (5).

3.2. SAT-Based Demodulation

With the continuous-time SAT available, we can built either an analog or a digital demodulator. For the latter, one has to first sample $\hat{p}_R(t)$ and $r(t)$ and proceed as in any other digital receiver. However, to maintain the full energy in $p_R(t)$, we recommend demodulation using a SAT-based correlator. Specifically, we form the decision statistic $d(k) = \int_0^{T_R} \hat{p}_R(t) r(t+\hat{\tau}_0+kT_s)dt$ using the $\hat{p}_R(t)$ and $\hat{\tau}_0$ obtained as in (9). Substituting $r(t)$ from (3), we can re-write $d(k)$ as

$$\begin{aligned} d(k) = &\sqrt{\mathcal{E}}\phi_{\hat{p}_R p_R}(0;\tilde{\tau}_0)s(k) + \eta(k;\tilde{\tau}_0) + \rho(k;\tilde{\tau}_0) \\ &+ \sqrt{\mathcal{E}} \sum_{n=-2(M-1), n\neq 0}^{2(M-1)} \phi_{\hat{p}_R p_R}(n;\tilde{\tau}_0)s(k+n) \end{aligned} \tag{10}$$

where $\tilde{\tau}_0 := \tau_0 - \hat{\tau}_0$, $\phi_{\hat{p}_R p_R}(n;\tilde{\tau}_0) := \int_0^{T_R} \hat{p}_R(t) p_R(t-nT_s - \tilde{\tau}_0)dt$, $\eta(k;\tilde{\tau}_0) := \int_0^{T_R} \hat{p}_R(t)\eta(t+kT_s+\hat{\tau}_0)dt$, and likewise for $\rho(k;\tilde{\tau}_0)$. Based on (10), Viterbi's Algorithm (VA), sphere decoding, or, linear equalization can be invoked depending on the application-specific tradeoff between BER and affordable complexity. For UWB receivers, where (sub-)chip rate sampling is prohibitive, VA applied to $d(k)$ is the only ML optimal (in the absence of MUI) UWB receiver based on symbol-rate samples.

To further reduce complexity, one can absorb the ISI and MUI plus AWGN terms in (10) into a single colored noise term and proceed with a low-complexity (albeit sub-optimal) slicer. In UWB single- or multi-user access with binary symbol transmissions this amounts to demodulating symbols with the sign detector:

$$\hat{s}(k) = \mathsf{sign}\left[\int_0^{T_R} \hat{p}_R(t) r(t+\hat{\tau}_0+kT_s)dt\right] \, . \tag{11}$$

Summarizing our result in this section, we have:

Proposition 2: *Both during and after the synchronization phase, ML optimal, linear equalization and low-complexity matched filter options are available for demodulating* $s(k)$ *from the decision statistic in (10) that is based on the MUI- and ISI-resilient SAT and timing estimated blindly under C1-C4 as in (9).*

4. LARGE SAMPLE PERFORMANCE ANALYSIS

Starting with $\bar{r}(t)$ in (5), it is easy to check that the conditions for applying the law of large numbers in [10] are satisfied here, ensuring that $\bar{r}(t)$ is mss consistent; i.e., $\lim_{N\to\infty} \bar{r}(t) \overset{mss}{=} \mathsf{E}r(t)$ for $t \in [0, MT_s]$. Since well behaved functions of consistent estimators are themselves consistent, the latter implies that $\lim_{N\to\infty}\hat{\tau}_0 \overset{mss}{=} \arg\max_{\tau\in[0,MT_s)} J(\tau) := \tau_0$ and $\lim_{N\to\infty}\hat{p}_R(t) \overset{mss}{=} p_R(t)$, meaning that $\hat{\tau}_0$ and $\hat{p}_R(t)$ are indeed mss consistent. In summary, we have :

Proposition 3: *The timing and SAT estimators in (9) are mss consistent. Asymptotically (as* $N\to\infty$*), the demodulator in (11) collects the maximum possible energy and thus upper bounds the BER performance of the RAKE receiver.*

Although the offset τ searched can be anywhere in $[0, MT_s)$, the mss consistency of $\hat{\tau}_0$ guarantees that we will be sufficiently close to the true τ_0 when N is sufficiently large. Conservatively, here we suppose $|\tau_0 - \hat{\tau}_0| \leq T_s$. Similarly, for large enough N, the estimated SAT will satisfy $\hat{p}_R(t) = (\sqrt{\mathcal{E}}\mu_0)^{-1}\mathsf{E}r(t+\hat{\tau}_0) = \sum_{k=-1}^{1} p_R(t + kMT_s - \tau_0 + \hat{\tau}_0)$ with $t\in[0,T_R]$. Considering $|\tau_0 - \hat{\tau}_0| \leq T_s$, only the summand corresponding to $k=0$ contributes, and we arrive at:

$$\hat{p}_R(t) = p_R(t-\tau_0+\hat{\tau}_0), \; t\in[0,T_R]. \tag{12}$$

Using (12) in eq. (10), we obtain $\phi_{\hat{p}_R p_R}(n;\tilde{\tau}_0) = \int_0^{T_R} p_R(t-\tilde{\tau}_0)p_R(t-nT_s-\tilde{\tau}_0)dt$. Notice that when $n\notin[-(M-2), M-2]$, we have $\phi_{\hat{p}_R p_R}(n;\tilde{\tau}_0) = 0$; while setting $n=0$, yields the energy captured by the estimated SAT that we define as: $E_C(\tilde{\tau}_0) := \int_0^{T_R} p_R^2(t-\tilde{\tau}_0)dt$. Let the noise subsume MUI, and abbreviate the sum in (10) as $ISI(k)$. Taking all these into account, the detection statistic implied by the mss consistency of $\hat{\tau}_0$ and $\hat{p}_R(t)$ for N sufficiently large, is given by:

$$d(k) = \sqrt{\mathcal{E}}E_C(\tilde{\tau}_0)s(k) + ISI(k) + \eta(k;\tilde{\tau}_0) \, , \tag{13}$$

where $\eta(k;\tilde{\tau}_0) := \int_0^{T_R} p_R(t-\tilde{\tau}_0)\eta(t+kT_s+\hat{\tau}_0)dt$ is zero mean Gaussian with variance $E_C(\tilde{\tau}_0)N_0/2$. Notice that $ISI(k)$ is a finite-valued random variable since it involves $2(M-2)$ random symbols: $\{s(k+n), \; n\in[-M+2, M-2], \; n\neq 0\}$. When $s(k)$ is binary, the BER is given by the well known simple closed-form in terms of the Gaussian tail (Q) function:

$$P_e = 2^{-2(M-2)} \sum_{ISI(k)\in\mathcal{A}_{ISI}} Q\left(\sqrt{\frac{2\mathcal{E}E_C}{N_0}} + \sqrt{\frac{2}{E_C N_0}}ISI(k)\right), \tag{14}$$

where $\mathcal{A}_{ISI}$ denotes the finite alphabet of the $ISI(k)$ term. As an immediate corollary of (14), we can set $M=2$ and find the BER for the ISI-free case with BPSK: $P_e = Q(\sqrt{2\mathcal{E}E_C/N_0})$. Although explicit forms are shown here only for BPSK, the general result is as follows:

Proposition 4: *For* N *large enough to ensure* $|\tau_0 - \hat{\tau}_0| \leq T_s$*, the BER incurred by the SAT-based slicer (11) in the presence of zero-mean AWGN is computable and depends on the severity of ISI and the energy captured by the estimated SAT. For binary constellations, the BER is given by (14).*

A point worth emphasizing is the BER dependence on the energy capture $E_C(\tilde{\tau}_0)$ that matters more than the accuracy of $\hat{\tau}_0$. Indeed, even when the error $\tilde{\tau}_0$ is relatively high, if E_C captures most

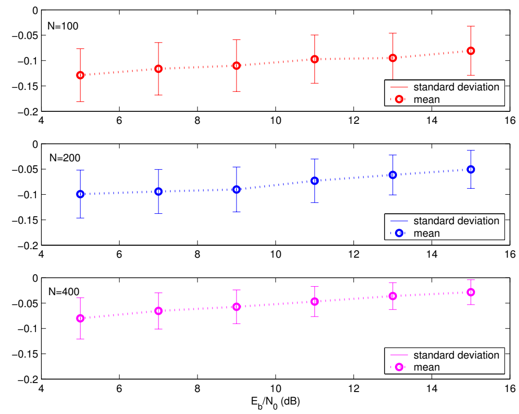

Fig. 3. Normalized (with respect to T_s) mean $\pm$ half of the standard deviation of the timing estimation errors when both MUI and ISI are present (MUI is caused by two asynchronous nodes with the same power).

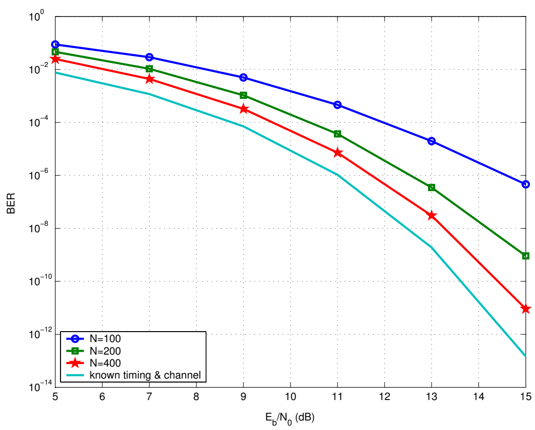

Fig. 4. BER performance when both MUI and ISI are present.

of the E_R energy, the resultant BER will be low; see also [1]. This is important since after all the goal is reliable demodulation rather than "super-accurate" synchronization.

5. SIMULATIONS

In this section, we simulate the synchronization and demodulation schemes of Section 3 in the most challenging scenario where both ISI and MUI are present. We will adopt BPSK symbols to modulate the so called Gaussian (monocycle) pulse shaper $p(t) = 2\sqrt{e}A(t/\tau_g)$ $\exp(-2t^2/\tau_g^2)$ with $\tau_g = 0.2$ ns; in asymmetric BPSK, we use $\theta = 3$. The multipath channel is "CM 1" from the IEEE 802.15.3a working group [11], whose delay spread is upper bounded by 30 ns. Simulated performance curves are obtained by averaging 1000 Monte Carlo runs. We select $T_f = 10$ns, $N_f = 10$ and $T_c = 1$ns to induce ISI. Spreading codes $\{c_k\}_{k=0}^{9}$ are randomly generated taking values of $\{0, 1, ..., 9\}$. Using $M = 3$ in C2, the results of implementing (9) and (11) are depicted in Figs. 3 and 4 respectively.

From the simulations, one can verify that with reasonable averaging (N), our SAT receiver will be only $1 - 2$dBs away from the clairvoyant one (with perfectly known timing and channel).

6. CONCLUSIONS

We derived a transmission protocol along with ISI- and MUI- resilient receiver algorithms for low-complexity blind timing acquisition and demodulation based on a synchronized aggregate template (SAT). The latter captures transmit-filter, ISI and unmodeled receiver effects, all of which are allowed to be unknown. Our novel blind SAT receiver offers not only robustness relative to the popular RAKE receiver, but also exhibits improved performance at lower complexity because it avoids the approximation emerging with a reduced number of RAKE fingers while at the same time it completely avoids estimation of the channel taps and delays needed when designing a RAKE receiver. We also revealed that for sufficiently long averaging times, what matters is the energy captured in the SAT and not necessarily the accuracy of the timing estimate itself. It is worth mentioning that our algorithms find universal applicability to a broad spectrum of narrowband, wideband or UWB modalities transmitted over AWGN or ISI-inducing wireless multi-access channels.

7. REFERENCES

[1] Z. Tian and G. B. Giannakis, "BER sensitivity to mis-timing in ultra-wideband communications," *IEEE Trans. on Signal Processing*, 2004 (to appear).

[2] D. Porrat and D. Tse, "Bandwidth Scaling in Ultra Wideband Communication," in *Proc. of 41st Allerton Conf.*, Univ. of Illinois at U-C, Monticello, IL, October 1-3, 2003.

[3] E. A. Homier and R. A. Scholtz, "Rapid acquisition of ultra-wideband signals in the dense multi-path channels," in *Proc. of UWBST*, Baltimore, MD, pp. 105-110, May 20-23, 2002.

[4] V. Lottici, A. D. Andrea, and U. Mengali, "Channel estimation for ultra-wideband communications," *IEEE J. Select. Areas Commun.*, vol. 20, pp. 1638-1645, Dec. 2002.

[5] Z. Wang and X. Yang, "Ultra wide-band communications with blind channel estimation based on first-order statistics," in *Proc. of ICASSP*, Montreal, Quebec, Canada, May 2004.

[6] L. Yang and G. B. Giannakis, "Blind UWB timing with a dirty template," in *Proc. of ICASSP*, Montreal, Quebec, Canada, May 2004.

[7] Z. Tian and G. B. Giannakis, "A GLRT Approach to Data-Aided Timing Acquisition in UWB Radios - Parts I and II," *IEEE Trans. Wirel. Commun.*, 2005 (to appear).

[8] L. Yang and G. B. Giannakis, "Ultra-wideband communications: an idea whose time has come," *IEEE Signal Processing Magazine*, Nov. 2004.

[9] X. Luo and G. B. Giannakis, "Low-complexity blind synchronization and demodulation for (ultra-) wideband multi-user ad hoc access," submitted to *IEEE Trans. Wirel. Commun.*, Sep. 2004.

[10] A. V. Dandawate and G. B. Giannakis, "Asymptotic theory of mixed time averages and kth-order cyclic moment and cumulant statistics," *IEEE Trans. Inf. Theory*, vol. 41, pp. 216-232, Jan. 1995.

[11] IEEE P802.15 Working Group for WPANs, *Channel Modeling Sub-Committee Report Final*, IEEE P802.15-02/368r5-SG3a, Nov. 2002.